Calculation of the one-point Green's function for a $-g\phi^4$ quantum field theory

Carl M. Bender,* Peter N. Meisinger,† and Haitang Yang‡
Department of Physics, Washington University, St. Louis, Missouri 63130
(Received 7 June 2000; published 11 January 2001)

It has recently been shown that, when properly defined, a $-gx^4$ potential in quantum mechanics possesses a positive definite spectrum. The positivity of the spectrum is apparently due to the $\mathcal{PT}$ symmetry of the Hamiltonian. Furthermore, for such a theory the expectation value $\langle x\rangle$ is *not* zero. This paper extends these results to a $-g\phi^4$ quantum field theory in D-dimensional Euclidean space. The value of the one-point Green's function $G_1=\langle\phi\rangle$ in this field theory is calculated in the weak-coupling and strong-coupling regimes. Nonperturbative techniques must be used in both of these regimes. For small g, the value of G_1 is dominated by a classical soliton. Strong-coupling graphical methods are used to calculate G_1 for large g.

DOI: 10.1103/PhysRevD.63.045001 PACS number(s): 11.10.Kk, 02.30.Mv, 11.10.Lm, 11.30.Er

I. INTRODUCTION

In 1952 Dyson argued heuristically that Rayleigh-Schrödinger perturbation theory for quantum electrodynamics is divergent [1]. This argument is quite general and applies to the quantum anharmonic oscillator, whose Hamiltonian is

$$H=\frac{1}{2}p^2+\frac{1}{2}m^2x^2+\frac{1}{4}gx^4 \quad (g>0). \tag{1.1}$$

The argument goes as follows: If the coupling constant g is replaced by $-g$, then the potential is no longer bounded below, so the resulting theory has no ground state. Thus, there is an abrupt transition in the ground-state energy $E_0(g)$ at $g=0$. If we represent $E_0(g)$ as a series in powers of g, this series must have a zero radius of convergence because $E_0(g)$ has a singularity at the origin $g=0$ in the complex-coupling-constant plane. Hence, perturbation theory must diverge for all $g\neq 0$. While the conclusion that the perturbation series diverges is correct [2], this heuristic argument is flawed because the spectrum of the Hamiltonian

$$H=\frac{1}{2}p^2+\frac{1}{2}m^2x^2-\frac{1}{4}gx^4 \quad (g>0) \tag{1.2}$$

is ambiguous. This ambiguity is due to the absence of well-specified boundary conditions that the wave functions must satisfy. As we will see, the spectrum depends crucially on how this Hamiltonian with a negative coupling constant is obtained.[1]

There are many ways to obtain the Hamiltonian (1.2). For example, one can substitute $g=|g|e^{i\theta}$ into the Hamiltonian (1.1) and rotate from $\theta=0$ to $\theta=\pi$. Under this rotation, the ground-state energy $E_0(g)$ becomes complex [2,3]. Evidently, $E_0(g)$ is real and positive when $g>0$ and complex when $g<0$.[2] One can also obtain Eq. (1.2) as a limit of the Hamiltonian

$$H=\frac{1}{2}p^2+\frac{1}{2}m^2x^2+\frac{g}{2+\alpha}x^2(ix)^\alpha \quad (g>0) \tag{1.3}$$

as $\alpha:0\to 2$. Recently, Hamiltonians like that in Eq. (1.3) have been studied in great detail [4–15]. It has been shown that for $\alpha\geqslant 0$ the spectra of such Hamiltonians are real, positive, and discrete. The spectrum of the limiting Hamiltonian (1.2) obtained in this manner is similar to that of the Hamiltonian in Eq. (1.1); it is entirely real, positive, and discrete. [The positive energy eigenvalues of the two Hamiltonians (1.1) and (1.2) are numerically different.]

How can one Hamiltonian (1.2) possess two such astonishingly different spectra? The answer lies in the boundary conditions satisfied by the wave functions $\psi_n(x)$. In the first case, in which $\theta=\arg g$ is rotated in the complex-g plane from 0 to π, $\psi_n(x)$ vanishes in the complex-x plane as $|x|\to\infty$ inside the wedges $-\pi/3<\arg x<0$ and $-4\pi/3<\arg x<-\pi$ [16]. In the second case, in which the exponent α ranges from 0 to 2, $\psi_n(x)$ vanishes in the complex-x plane as $|x|\to\infty$ inside the wedges $-\pi/3<\arg x<0$ and $-\pi<\arg x<-2\pi/3$ [4,5]. In this second case the boundary conditions hold in wedges that are symmetric with respect to the imaginary axis. The boundary conditions enforce the $\mathcal{PT}$ symmetry of the Hamiltonian, and evidently are responsible for the reality of the energy spectrum [5].

There is another striking difference between the two theories corresponding to the Hamiltonian (1.2). We define the one-point Green's function $G_1(g)$ [the expectation value of the operator x with respect to the ground-state wave function $\psi_0(x)$] by the ratio of integrals

*Email address: cmb@howdy.wustl.edu
†Email address: pnm@howdy.wustl.edu
‡Email address: hyangb@artsci.wustl.edu

[1]One question that may occur to the reader is whether the eigenfunctions of Eq. (1.2) are analytic continuations of the eigenfunctions of the usual anharmonic oscillator (1.1). The answer to this question is definitely not because the eigenfunctions satisfy totally different boundary conditions.

[2]If we rotate from $\theta=0$ to $\theta=-\pi$, then we obtain the same Hamiltonian as in Eq. (1.2) but the spectrum is the complex conjugate of the spectrum obtained when we rotate from $\theta=0$ to $\theta=\pi$.

$$G_1(g)=\frac{\langle 0|x|0\rangle}{\langle 0|0\rangle}\equiv\frac{\int_C dx\, x\psi_0^2(x)}{\int_C dx\, \psi_0^2(x)}, \tag{1.4}$$

where the contour C is a path in the complex-x plane that lies in the asymptotic wedges described above. The value of $G_1(g)$ for the Hamiltonian H in Eq. (1.2) depends on the limiting process by which we obtain H. If we use a rotation in which we substitute $g=g_0e^{i\theta}$ into the Hamiltonian (1.1) and rotate from $\theta=0$ to $\theta=\pi$, we find by an elementary symmetry argument that $G_1(g)=0$ for all g on the semicircle in the complex-g plane. Evidently, this rotation in the complex-g plane preserves parity symmetry (reflection through the origin, $x\to -x$). There is no parity symmetry breaking for the Hamiltonian defined in this manner. However, if we define H in Eq. (1.2) by using the Hamiltonian in Eq. (1.3) and by taking the limit as α ranges from 0 to 2, we find that $G_1(g)\neq 0$. Indeed, $G_1(g)$ is nonvanishing for *all* values of $\alpha>0$. Thus, in this theory, while $\mathcal{PT}$ symmetry (reflection about the imaginary axis, $x\to -x^*$) is preserved, parity symmetry is permanently broken.

These two different results for $G_1(g)$ emphasize the ambiguity in Dyson's argument and show that the boundary conditions in the integrals in Eq. (1.4) are crucial for determining the one-point Green's function. We are concerned in this paper with the theory that preserves $\mathcal{PT}$ symmetry. In this theory the energy spectrum is real and $G_1(g)$ is nonzero.

The purpose of this paper is to extend these quantum-mechanical arguments to the quantum field theory whose D-dimensional Euclidean space Lagrangian density is

$$\mathcal{L}=\frac{1}{2}(\nabla\phi)^2+\frac{1}{2}m^2\phi^2-\frac{g}{4}\phi^4. \tag{1.5}$$

What is remarkable about this ''wrong-sign'' field theory is that, when it is obtained using the $\mathcal{PT}$-symmetric limit, the energy spectrum is real and positive, and the one-point Green's function is nonzero [17–20]. Furthermore, the field theory is renormalizable, and in four dimensions is asymptotically free (and thus nontrivial). Based on these features of the theory, we believe that the theory may provide a useful setting to describe the Higgs particle [21].

While the Lagrangian (1.5) is not Hermitian, it is invariant under $\mathcal{PCT}$ reflections. Conventional field-theoretic Lagrangians possess two crucial symmetries, the continuous symmetry of the proper Lorentz group and the discrete symmetry of Hermiticity. While Lorentz invariance is a physical requirement, Hermiticity is a useful but rather mathematical constraint. However, from the assumptions of Lorentz invariance and positivity of the spectrum of the Lagrangians one can prove the $\mathcal{PCT}$ theorem and thereby establish the very physical symmetry of $\mathcal{PCT}$ invariance. The constraint of $\mathcal{PCT}$ invariance is weaker than Hermiticity, so Lagrangians having this property need not be Hermitian. In quantum mechanics and in a scalar quantum field theory like that defined in the Lagrangian (1.5), the $\mathcal{C}$ operator is unity, so $\mathcal{PCT}$ symmetry reduces to $\mathcal{PT}$ symmetry. While it has not yet been proved, there is strong analytical and numerical evidence supporting the conjecture that the energy levels of the Hamiltonians constructed from such Lagrangians are all real and positive. The reality and positivity of the spectrum is apparently a consequence of the $\mathcal{PT}$ symmetry of $\mathcal{L}$.

This paper is organized as follows. In Sec. II we show how to calculate the one-point Green's function in the weak-coupling limit. We begin with the simplest case of a zero-dimensional field theory and show that Feynman diagrams cannot be used to calculate G_1. Next, we perform a detailed calculation of G_1 in one dimension (quantum mechanics). We then extend this calculation to quantum field theory in D-dimensional Euclidean space. In Sec. III we show how to calculate G_1 using strong-coupling lattice techniques and determine G_1 as a series in inverse powers of the coupling constant g.

II. WEAK-COUPLING CALCULATION OF G_1

In this section we perform a weak-coupling (small-g) calculation of the one-point Green's function G_1, which is defined as a *complex* functional integral in Euclidean space:

$$G_1=\frac{\int_C \mathcal{D}\phi\,\phi(0)e^{-L[\phi]}}{\int_C \mathcal{D}\phi\, e^{-L[\phi]}}. \tag{2.1}$$

Here, $L[\phi]=\int d^Dx\,\mathcal{L}$ with $\mathcal{L}$ given in Eq. (1.5) and C is a contour in the complex-ϕ plane. We define the contour C as follows: The functional integrals in Eq. (2.1) must be regarded as an infinite product of ordinary integrals, one integral for each lattice point in Euclidean space. For each of these ordinary integrals the contour of integration must lie within 45° wedges that lie in the lower-half plane and are centered about the $-45°$ and $-135°$ lines. These two wedges are symmetrically placed about the imaginary axis.

A. Feynman rules

We begin by pointing out that if we attempt to calculate the integrals in Eq. (2.1) using Feynman rules, we obtain the incorrect result that G_1 vanishes. To derive the Feynman rules for evaluating the integral in Eq. (2.1) we introduce a source term $J(x)$ and consider the functional-integral representation for the vacuum persistence amplitude $Z[J]$:

$$Z[J]=\int_C \mathcal{D}\phi\exp\left(-\int d^Dx\left\{\frac{1}{2}[\nabla\phi(x)]^2+\frac{1}{2}m^2\phi^2(x)-\frac{1}{4}g\phi^4(x)-J(x)\phi(x)\right\}\right). \tag{2.2}$$

This expression for $Z[J]$ may be rewritten as

$$Z[J]=\exp\left[\frac{1}{4}g\int d^Dx\,\frac{\delta^4}{\delta J(x)^4}\right]\times\int_C \mathcal{D}\phi\,\exp\left(-\int d^Dx\left\{\frac{1}{2}[\nabla\phi(x)]^2+\frac{1}{2}m^2\phi^2(x)-J(x)\phi(x)\right\}\right). \tag{2.3}$$

To evaluate the Gaussian functional integral we deform the contour C so that it lies on the real axis in function space.[3] We then evaluate the standard Gaussian integral,

$$Z[J]=\mathcal{N}\exp\left[\frac{1}{4}g\int d^Dx\,\frac{\delta^4}{\delta J(x)^4}\right]\times\exp\left[\frac{1}{2}\int d^Dx\int d^Dy\,J(x)\Delta(x-y)J(y)\right], \tag{2.4}$$

where $\mathcal{N}$ is an infinite constant and $\Delta(x)$ is the Euclidean coordinate-space propagator:

$$\Delta(x)=(2\pi)^{-D/2}\left(\frac{m}{|x|}\right)^{(D-2)/2}K_{(D-2)/2}(m|x|)=(2\pi)^{-D}\int\frac{d^Dp}{p^2+m^2}e^{ip\cdot x}. \tag{2.5}$$

From Eq. (2.4) we can read off the Feynman rules:

$$\begin{aligned}&6g \quad \text{for a vertex,}\\ &\Delta(x-y) \quad \text{for a line connecting } x \text{ to } y.\end{aligned} \tag{2.6}$$

If we naively employ these rules to calculate the one-point Green's function G_1, we obtain the result that $G_1=0$ to all orders in powers of g. This conclusion follows from the fact that the vertex is a *four*-point vertex, and thus no Feynman diagrams contribute to G_1. However, it is not correct to conclude that the one-point Green's function for this theory vanishes. Indeed, G_1 does not vanish, but rather is *exponentially small* as $g\to 0$. To calculate G_1 in this limit we must use *nonperturbative techniques.* We illustrate these techniques first for the case of a zero-dimensional quantum field theory.

B. Zero-dimensional case

In zero space-time dimensions Eq. (2.1) becomes a ratio of ordinary integrals:

$$G_1=\frac{\int_C dx\,x e^{-L(x)}}{\int_C dx\,e^{-L(x)}}, \tag{2.7}$$

where $L(x)=\frac{1}{2}m^2x^2-\frac{1}{4}gx^4$. Here, C is a contour whose end points lie inside 45° wedges in the complex-x plane as described above.

We transform to dimensionless variables by setting $x=mt/\sqrt{g}$:

$$G_1=\frac{m}{\sqrt{g}}\,\frac{\int_C dt\,te^{-\Lambda(t)/\epsilon}}{\int_C dt\,e^{-\Lambda(t)/\epsilon}}, \tag{2.8}$$

where $\epsilon=gm^{-4}$ and $\Lambda(t)=\frac{1}{2}t^2-\frac{1}{4}t^4$.

For small positive ϵ we use the saddle-point method [22] to approximate the integrals. To find the saddle points we differentiate $\Lambda(t)$ and get $\Lambda'(t)=t-t^3$. The algebraic equation $\Lambda'(t)=0$ gives three saddle points at $t=0$ and $t=\pm 1$. The second derivative of $\Lambda(t)$ determines the local directions of the steepest curves emanating from the saddle points. Since $\Lambda''(t)=1-3t^2$, we see that the steepest-descent paths at $t=0$ lie on the positive- and negative-real axes, while the steepest-descent paths at $t=\pm 1$ point in the positive- and negative-imaginary directions. We must deform the original contour C into a steepest contour. This steepest contour runs along a curve from $t=\infty e^{-3\pi i/4}$ and enters the saddle point at $t=-1$ vertically. It leaves this saddle point and goes along the real axis, through the saddle point at $t=0$, and continues on to the saddle point at $t=1$. It emerges from this saddle point going vertically downward and curves off to $t=\infty e^{-\pi i/4}$. The maximum value of the integrand on this curve is at $t=0$. Note that the endpoints of the steepest-descent contour lie in the centers of the wedges of convergence.

The integral in the denominator of Eq. (2.8) is dominated by the *perturbative* saddle point at $t=0$; that is, when we expand about this point, we obtain a series in powers of ϵ whose terms can be represented as a sum of conventional Feynman diagrams. The leading term in the expansion of this integral is $\sqrt{2\pi\epsilon}$. However, the saddle point at $t=0$ does not contribute to the integral in the numerator. Indeed, the integral along the steepest path joining $t=-1$ to $t=1$ vanishes because the integrand is odd. The contributions to the integral in the numerator come from the portions of the steepest-descent paths lying infinitesimally below the saddle points at $t=\pm 1$. To leading order, these two contributions are $-i\sqrt{\pi\epsilon}e^{-1/(4\epsilon)}$. Substituting these results into Eq. (2.8), we obtain the final answer

$$G_1\sim-\frac{i}{m}2^{-1/2}\epsilon^{-1/2}e^{-1/(4\epsilon)}\quad(\epsilon\to 0^+). \tag{2.9}$$

We will extend this saddle-point calculation to the general D-dimensional functional integral (2.1), but this calculation

[3]This deformation is valid because the Gaussian integral converges for C lying in wedges of angular opening 90° centered about the positive and negative real axes in the complex-ϕ plane. We choose the contour C so that it lies in the region common to the 45° wedge in which the original functional integral for $Z[J]$ converges and the 90° wedge in which the Gaussian functional integral converges.

is nontrivial. Thus, as a guide, we consider the special quantum-mechanical case corresponding to $D=1$ first. For this case we can obtain the small-g asymptotic behavior of G_1 directly from the Schrödinger equation.

C. One-dimensional case

In this subsection we calculate G_1, which is defined in Eq. (1.4) as the ratio of integrals $G_1=\int_C dx\, x\psi_0^2(x)/\int_C dx\, \psi_0^2(x)$, where $\psi_0(x)$ is the ground-state wave function satisfying the Schrödinger equation

$$-\frac{1}{2}\psi_0''(x)+\left(\frac{1}{2}m^2x^2-\frac{1}{4}gx^4\right)\psi_0(x)=E\psi_0(x) \tag{2.10}$$

and E is the ground-state energy. The contour of integration C lies inside 60° wedges lying in the lower-half plane and adjacent to the positive and negative real axes. This is the quantum-mechanical analogue of Eq. (2.1).

We convert the Schrödinger equation to dimensionless form by letting

$$x=\frac{t}{\sqrt{m}},\quad g=\epsilon m^3,\quad E=\lambda m, \tag{2.11}$$

so that t, ϵ, and λ are all dimensionless quantities. In terms of these new variables,

$$G_1=\frac{1}{\sqrt{m}}\frac{\int_C dt\, ty^2(t)}{\int_C dt\, y^2(t)}, \tag{2.12}$$

where $y(t)$ satisfies the dimensionless Schrödinger equation

$$-\frac{1}{2}y''(t)+\left(\frac{1}{2}t^2-\frac{1}{4}\epsilon t^4\right)y(t)=\lambda y(t). \tag{2.13}$$

The Feynman rules for this theory are valid as long as they do not predict that a quantity vanishes. Therefore, the ground-state energy λ is given by $\lambda=\frac{1}{2}+\mathrm{O}(\epsilon)$. Here, the order ϵ term is obtained by evaluating the lowest-order graph (a figure-8 graph with one vertex). To zeroth order in ϵ the ground-state wave function is

$$y(t)=e^{-t^2/2}[1+\mathrm{O}(\epsilon)]. \tag{2.14}$$

Thus, to zeroth order in ϵ the norm of the ground state is

$$\int_{-\infty}^{\infty}dt\, y^2(t)=\int_{-\infty}^{\infty}dt\, e^{-t^2}[1+\mathrm{O}(\epsilon)]=\sqrt{\pi}[1+\mathrm{O}(\epsilon)]. \tag{2.15}$$

This yields, to leading order in ϵ,

$$G_1=\frac{1}{\sqrt{m\pi}}\int_C dt\, ty^2(t). \tag{2.16}$$

The integral in this last expression vanishes to all orders in ϵ because to each order in powers of ϵ, the ground-state wave function $y(t)$ is an even function. Thus, conventional perturbation theory gives 0 for G_1. Yet as we saw in the previous subsection, it is not 0; rather, it is exponentially suppressed. This suppression occurs because the correction to $y(t)$ at zeroth order is exponentially small.

To find the correction to $y(t)$ we partition the real-t axis into three regions, which are defined in terms of the turning points at $\pm t_1$ and at $\pm t_2$, where t_1 and t_2 are the zeros of $\phi(t)=t^2-\frac{1}{2}\epsilon t^4-1$. To first order in ϵ we have

$$t_1=1+\frac{\epsilon}{4}+\mathrm{O}(\epsilon^2), \tag{2.17}$$

which is a distance of order 1 from the origin $t=0$. Also,

$$t_2=\sqrt{2/\epsilon}\left[1-\frac{\epsilon}{4}+\mathrm{O}(\epsilon^2)\right], \tag{2.18}$$

which is far from the origin.

Region I includes all t that are of order 1 (including the point t_1). All values of t in this region must be small compared with $\epsilon^{-1/4}$. Uniformly in this region we can neglect the term ϵt^4 compared with t^2-1. The solution to the Schrödinger equation in this region is just $y(t)=e^{-t^2/2}$, where we have chosen the normalization $y(0)=1$.

Region II includes those values of t that are large compared with 1 but are small compared with t_2 (far enough from t_2 so that the WKB solution is still valid). In region II we can solve the Schrödinger equation using the WKB solution because $\phi(t)\gg 1$. (This asymptotic inequality is equivalent to the condition that $\hbar$ be small.) The leading-order WKB solution that falls off exponentially has the explicit form

$$y_{\mathrm{WKB}}(t)=C[\phi(t)]^{-1/4}\exp\left[-\int_{t_1}^{t}ds\,\sqrt{\phi(s)}\right]. \tag{2.19}$$

The overlap of regions I and II consists of those values of t that satisfy $t\gg 1$ and $t\ll\epsilon^{-1/4}$. In this overlap region the asymptotic approximation to the leading-order WKB solution is

$$y_{\mathrm{WKB}}(t)\sim C\sqrt{2}e^{-t^2/2}\quad (t\gg 1,\ t\ll\epsilon^{-1/4}). \tag{2.20}$$

An asymptotic match with $y(t)$ in region I implies that $C=1/\sqrt{2}$.

Region III is defined as those values of t that are in the vicinity of t_2. Specifically, we let $t=t_2(1-\epsilon^{2/3}r/2)$, where $r\ll\epsilon^{-2/3}$. In terms of the variable r the dimensionless Schrödinger equation becomes the Airy equation $y''(r)=ry(r)$, whose general solution is

$$y_{\mathrm{III}}(r)=C_1\mathrm{Ai}(r)+C_2\mathrm{Bi}(r). \tag{2.21}$$

For large positive r, $\mathrm{Ai}(r)$ decays exponentially as r increases

$$\mathrm{Ai}(r)\sim\frac{1}{2\sqrt{\pi}}r^{-1/4}e^{-2r^{3/2}/3}\quad(r\gg1),\tag{2.22}$$

while $\mathrm{Bi}(r)$ decays exponentially as r increases:

$$\mathrm{Bi}(r)\sim\frac{1}{\sqrt{\pi}}r^{-1/4}e^{2r^{3/2}/3}\quad(r\gg1).\tag{2.23}$$

Thus, in the overlap of regions II and III, which consists of those r satisfying the asymptotic inequalities $r\gg1$ and $r\ll\epsilon^{-2/3}$,

$$y_{\mathrm{III}}(r)\sim\frac{1}{\sqrt{\pi}}C_2r^{-1/4}e^{2r^{3/2}/3}.\tag{2.24}$$

Notice that this asymptotic behavior does not depend on C_1, but only on C_2. The C_1 contribution is subdominant.

Now we must approximate the WKB solution in the overlap of regions II and III. First, we have $\phi(t)\sim2^{1/4}\epsilon^{-1/12}r^{1/4}$ $(1\ll r\ll\epsilon^{-2/3})$. Second, we approximate $\int_{t_1}^{t}ds\,\sqrt{\phi(s)}$ by writing it as the difference of two integrals:

$$\int_{t_1}^{t}ds\,\sqrt{\phi(s)}=\int_{t_1}^{t_2}ds\,\sqrt{\phi(s)}-\int_{t}^{t_2}ds\,\sqrt{\phi(s)}.\tag{2.25}$$

The first of these integrals is evaluated in Eq. (4.24) of Ref. [3]

$$\int_{t_1}^{t_2}ds\,\sqrt{\phi(s)}\sim\frac{2}{3\epsilon}-\frac{1}{4}\left[\log\left(\frac{32}{\epsilon}\right)+1\right].\tag{2.26}$$

We evaluate the second of these integrals by making the changes of variable $t=\sqrt{2/\epsilon}\,(1-\frac{1}{2}\epsilon^{2/3}r)$ and $s=\sqrt{2/\epsilon}\,(1-\frac{1}{2}\epsilon^{2/3}\sigma)$. This gives

$$\int_{t}^{t_2}ds\,\sqrt{\phi(s)}\sim\int_{0}^{r}d\sigma\,\sqrt{\sigma}=\frac{2}{3}r^{3/2}.\tag{2.27}$$

Combining these results we obtain the asymptotic behavior of $y_{\mathrm{WKB}}(r)$ in the overlap of regions II and III:

$$y_{\mathrm{WKB}}(r)\sim2^{-3/4}\epsilon^{1/12}r^{-1/4}\exp\left[\frac{2}{3}r^{3/2}-\frac{2}{3\epsilon}+\frac{1}{4}\log\left(\frac{32}{\epsilon}\right)+\frac{1}{4}\right]\quad(1\ll r\ll\epsilon^{-2/3}).\tag{2.28}$$

Matching the asymptotic approximation (2.28) of the WKB solution in the overlap of regions II and III to the asymptotic approximation (2.24) of $y_{\mathrm{III}}(r)$ gives the value of C_2: $C_2=\sqrt{2\pi}\,e^{1/4}\epsilon^{-1/6}e^{-2/(3\epsilon)}$. We thus conclude that

$$y_{\mathrm{III}}(r)=C_1\mathrm{Ai}(r)+\sqrt{2\pi}e^{1/4}\epsilon^{-1/6}e^{-2/(3\epsilon)}\mathrm{Bi}(r).\tag{2.29}$$

We emphasize again that C_1 is not determined by this asymptotic match.

The constant C_1 is determined by the condition that the wave function $y(t)$ decay exponentially as t emerges from the turning point at t_2 at an angle of $-60°$. In this direction $r=\rho e^{2\pi i/3}$, where ρ is real and positive. From the exact functional identity [23]

$$\mathrm{Bi}(\rho e^{2\pi i/3})-i\,\mathrm{Ai}(\rho e^{2\pi i/3})=-2ie^{\pi i/3}\mathrm{Ai}(\rho)\tag{2.30}$$

we obtain the value of C_1. Thus,

$$y_{\mathrm{III}}(r)=\sqrt{2\pi}e^{1/4}\epsilon^{-1/6}e^{-2/(3\epsilon)}[\mathrm{Bi}(r)-i\,\mathrm{Ai}(r)].\tag{2.31}$$

For any other value of C_1, as ρ gets large and positive there is an admixture of $\mathrm{Bi}(\rho)$ which grows exponentially like $e^{2\rho^{3/2}/3}$ and violates the normalization condition.

By oddness, the integral for G_1 vanishes in the region between $-t_2$ and t_2. It remains to evaluate this integral from t_2 to ∞ along a path of positive ρ. Define

$$I_{\mathrm{right}}=\int_{t_2}^{\infty e^{-i\pi/6}}dt\,t\,y^2(t).\tag{2.32}$$

Next, we make the change of variable $t=\sqrt{2/\epsilon}\,(1-\epsilon^{2/3}r/2)$. This yields

$$I_{\mathrm{right}}=-\epsilon^{-1/3}\int_{0}^{\infty e^{2i\pi/3}}dr\,[\sqrt{2\pi}e^{1/4}\epsilon^{-1/6}e^{-2/(3\epsilon)}]^2\times[\mathrm{Bi}(r)-i\,\mathrm{Ai}(r)]^2,\tag{2.33}$$

where we have rotated the contour so that it follows the anti-Stokes line (the path of steepest descent) and we have replaced t in the integrand by t_2.

Next, we make the change of variable $r=e^{2\pi i/3}\rho$, where $\rho:0\to\infty$. This converts Eq. (2.33) to a real integral:

$$I_{\mathrm{right}}=-2\pi\epsilon^{-2/3}e^{1/2}e^{-4/(3\epsilon)}e^{2\pi i/3}\int_{0}^{\infty}d\rho\,[-2ie^{i\pi/3}\mathrm{Ai}(\rho)]^2,\tag{2.34}$$

where we have used the functional identity (2.30). The Airy function integral is evaluated by using the identity $\mathrm{Ai}^2(\rho)=[\rho\mathrm{Ai}^2(\rho)-\mathrm{Ai}'^2(\rho)]'$. Finally, using $\mathrm{Ai}'(0)=-3^{-1/3}/\Gamma(1/3)$, we obtain

$$I_{\mathrm{right}}=-4\pi\sqrt{e}\,\epsilon^{-2/3}e^{-4/(3\epsilon)}3^{-2/3}(1+i\sqrt{3})/\Gamma^2(1/3).\tag{2.35}$$

Adding together the right and left integrals that contribute to G_1, we note that the real parts cancel while the imaginary parts add. This gives a *negative imaginary* value for G_1:

$$G_1\sim-\frac{i}{\sqrt{m}}8\sqrt{\pi e}\,\epsilon^{-2/3}e^{-4/(3\epsilon)}3^{-1/6}/\Gamma^2(1/3)\quad(\epsilon\to0^+),\tag{2.36}$$

where we have used Eq. (2.16). Numerically, we have

$$G_1 \sim -\frac{i}{\sqrt{m}}(2.71248)\epsilon^{-2/3}e^{-4/(3\epsilon)} \quad (\epsilon \to 0^+). \tag{2.37}$$

This result for the asymptotic behavior of G_1 for small g is similar in form to that in Eq. (2.9) for the case $D=0$.

D. D-dimensional case

In this subsection we generalize the steepest-descent calculation done in Sec. II B to the case of D dimensions. We will use functional-integral techniques to find the controlling factor (the exponential contribution) of the asymptotic behavior of G_1 for arbitrary dimension D. (The full asymptotic behavior is much more difficult to obtain.) We begin with the one-point Green's function defined in Eq. (2.1).

We introduce dimensionless variables t, ϵ, and f as follows:

$$x = t/\sqrt{m}, \quad g = m^{4-D}\epsilon \quad \phi(x) = m^{(D-2)/2}\epsilon^{-1/2}f(t). \tag{2.38}$$

In terms of these new variables the expression for G_1 in Eq. (2.1) becomes

$$G_1 = \frac{m^{(D-2)/2}}{\sqrt{\epsilon}} \frac{\int_C \mathcal{D}f\, f(0) e^{-\Lambda[f]/\epsilon}}{\int_C \mathcal{D}f\, e^{-\Lambda[f]/\epsilon}}, \tag{2.39}$$

where the dimensionless Lagrangian $\Lambda[f]$ is

$$\Lambda[f] = \int d^D t \left\{ \frac{1}{2}[\nabla f(t)]^2 + \frac{1}{2}f^2(t) - \frac{1}{4}f^4(t) \right\}. \tag{2.40}$$

Next, we identify the saddle points contributing to the asymptotic behavior of the integrals in Eq. (2.39) as $\epsilon \to 0^+$. To do so we calculate the variational derivative of $\Lambda[f]$: $[\delta/\delta f(s)]\Lambda[f] = -\nabla^2 f(s) + f(s) - f^3(s)$. Based on our experience with the zero-dimensional calculation in Sec. II B and the one-dimensional calculation in Sec. II C, we expect that the solution to the equation $[\delta/\delta f(s)]\Lambda[f]=0$ will depend on whether we are interested in the integral in the numerator or in the denominator of Eq. (2.39). We expect that the *perturbative* saddle point $f(s)\equiv 0$ dominates the integral in the denominator. However, because of oddness, this saddle point does not contribute to the asymptotic expansion of the numerator.[4]

The asymptotic expansion of the integral in the numerator is dominated by a *soliton* defined by the boundary-value problem

$$-\nabla^2 f(s) + f(s) - f^3(s) = 0, \tag{2.41}$$

where $\lim_{|s|\to\infty} f(s) = 0$. We can obtain this soliton analytically only in the case $D=1$:

$$f_{D=1}(s) = \sqrt{2}\,\mathrm{sech}(s+C), \tag{2.42}$$

where C is an arbitrary constant of integration. Substituting this solution into the integral for $\Lambda[f]$ in Eq. (2.40), we obtain

$$\Lambda[f_{D=1}] = 4/3, \tag{2.43}$$

which reproduces the controlling factor $e^{-4/(3\epsilon)}$ of the small-ϵ asymptotic behavior in Eqs. (2.36) and (2.37).

In dimensions other than $D=1$ the controlling factor of the asymptotic behavior of G_1 for small ϵ has the form

$$G_1 \sim e^{-\Lambda[f]/\epsilon} \quad (\epsilon \to 0). \tag{2.44}$$

To find the value of $\Lambda[f]$ we seek a spherically symmetric solution[5] $f(r)$ to Eq. (2.41), where $r=|s|$. The function $f(r)$ then satisfies

$$-f''(r) - \frac{D-1}{r}f'(r) + f(r) - f^3(r) = 0 \quad (0 \leqslant r < \infty), \tag{2.45}$$

where $f(\infty)=0$. This boundary-value problem cannot be solved analytically, but numerical analysis gives for $\Lambda[f]$ the graph shown in Fig. 1. Note that the functional $\Lambda[f]$ passes through the calculated points $\frac{1}{4}$ at $D=0$ and $\frac{4}{3}$ at $D=1$. The curve rises to a maximum value between $D=3.5$ and $D=4$ and then starts to decrease. Some numerical values of $\Lambda[f]$ for various values of the Euclidean space-time dimension D are given in Table I.

The asymptotic formula in Eq. (2.44) is a geometrical-optics approximation. To obtain the complete leading-order asymptotic approximation to G_1 for small ϵ (the physical-optics approximation) we must expand about the soliton solution defined by Eq. (2.45). This is a nontrivial calculation for arbitrary D and we only discuss this calculation for the case $D=1$. To expand about the soliton solution for $D=1$ in Eq. (2.42) we substitute

$$f(t) = f_{D=1}(t) + \epsilon^{1/2}\eta(t) = \sqrt{2}\,\mathrm{sech}(t+C) + \epsilon^{1/2}\eta(t) \tag{2.46}$$

into the dimensionless action $\Lambda[f]$ in Eq. (2.40), where $\eta(t)$ represents fluctuations about the classical soliton $f_{D=1}(t)$. To zeroth order in powers of $\eta(t)$ the result is $\frac{4}{3}$, as we saw in Eq. (2.43). Also, terms linearly proportional to $\eta(t)$ vanish upon integration by parts because of the stationarity condition (2.41). Thus, we have

[4]The constant solutions $f(s)\equiv\pm 1$ do not contribute to the integrals in the numerator or the denominator of (2.39) because their action is infinite.

[5]We *assume* that the spherically symmetric solution minimizes the functional $\Lambda[f]$ in Eq. (2.40); this is equivalent to assuming that non-spherically symmetric solutions make subdominant contributions to the asymptotic behavior of G_1. In the massless case one can use Sobolev inequalities to justify using spherically symmetric solutions. In the massive case here we can only argue by analogy.

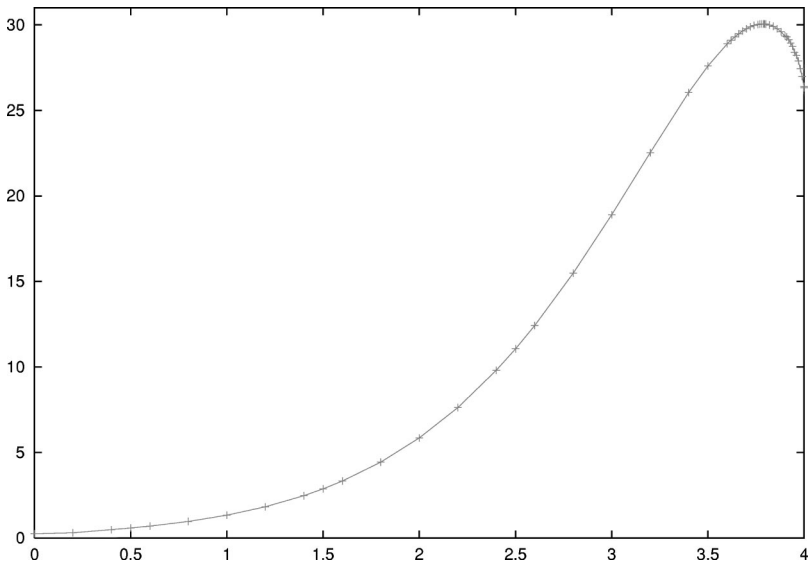

FIG. 1. Controlling factor (2.44) of the asymptotic behavior of the one-point Green's function G_1 for small dimensionless coupling constant ϵ. The controlling factor has the form $e^{-\Lambda[f]/\epsilon}$, which is nonperturbative in character. Plotted is the functional $\Lambda[f]$ versus the Euclidean space-time dimension D. At $D=0$ we have $\Lambda[f]=\frac{1}{4}$ and at $D=1$ we have $\Lambda[f]=\frac{4}{3}$, as calculated analytically. For other values of D we can only obtain $\Lambda[f]$ numerically. Some of the numerical values of $\Lambda[f]$ plotted here are given in Table I.

$$\Lambda[f_{D=1}+\epsilon^{1/2}\eta]=\frac{4}{3}+\frac{\epsilon}{2}\int dt\ \eta(t)M(t)\eta(t) - \epsilon^{3/2}\int dt\ f_{D=1}(t)\eta^3(t) - \frac{\epsilon^2}{4}\int dt\ \eta^4(t), \tag{2.47}$$

where the matrix $M(t)$ is the differential operator $M(t)=-d^2/dt^2+1-6\ \mathrm{sech}^2 t$.

The physical-optics correction to the geometrical-optics approximation in Eq. (2.44) requires that we evaluate the Gaussian functional integral

$$\int \mathcal{D}\eta \exp\left[-\frac{1}{2}\int dt\ \eta(t)M(t)\eta(t)\right]. \tag{2.48}$$

[Note that the small parameter ϵ has dropped out of this calculation because the term in Eq. (2.47) containing the operator M is proportional to ϵ and there is a factor of $1/\epsilon$ in the exponent in Eq. (2.39).] We know that the value of a Gaussian functional integral of the form (2.48) is the inverse of the square root of the product of the eigenvalues of M.

TABLE I. Numerical values of the dimensionless Lagrangian $\Lambda[f]$ in Eq. (2.40) for various values of the Euclidean space-time dimension D. Note that $\Lambda[f]$ rises to a maximum value between $D=3.5$ and $D=4$ and then starts to decrease. The function $\Lambda[f]$ is plotted as a function of D in Fig. 1.

D	$\Lambda[f]$	D	$\Lambda[f]$
0	1/4	3.0	18.9023
0.5	0.5853	3.5	27.6012
1.0	4/3	3.8	30.0387
1.5	2.8755	3.9	29.3452
2.0	5.8505	3.95	28.3897
2.5	11.0599	4.0	26.3209

To find the spectrum of M we must solve the Schrödinger equation

$$\left(-\frac{d^2}{dt^2}+1-6\ \mathrm{sech}^2 t\right)y(t)=Ey(t), \tag{2.49}$$

where E is the energy eigenvalue and $y(t)$ is the corresponding eigenfunction. The potential $1-6\ \mathrm{sech}^2 t$ has a minimum value of -5 and it levels off at 1 as $|t|\to\infty$. Therefore, there is a continuum spectrum beginning at $E=1$. There are also two normalizable bound states at $E=-3$ with corresponding eigenfunction $y(t)=\mathrm{sech}^2(t)$ and at $E=0$ with corresponding eigenfunction $y(t)=\mathrm{sech}(t)\tanh(t)$. The lowest-energy $(E=1)$ continuum eigenfunction is $y(t)=\mathrm{sech}^2(t)-\frac{2}{3}$, which is not normalizable.

The corresponding Gaussian functional integral to be evaluated in the denominator of Eq. (2.39) has the differential operator $M(t)=-d^2/dt^2+1$. The corresponding Schrödinger equation has a continuus spectrum beginning at $E=1$ and *no bound states*. Thus, the product of the eigenvalues of the continuum eigenstates cancels in the numerator and denominator and all that remains are the eigenvalues of the bound states. Because the lowest bound-state energy at $E=-3$ is *negative* and because we must take the square root of this eigenvalue, it is now clear why the one-point Green's function is imaginary, as we saw in Eq. (2.36).

Observe that the energy of the other bound state is *zero*. This implies that we cannot truncate the expansion in Eq. (2.47) at the Gaussian level. For this particular contribution we must retain the cubic term of order $\epsilon^{3/2}$. Thus, for this mode we must consider a cubic exponential integral of the form $\int d\eta \exp(-\sqrt{\epsilon}\,\eta^3)$. This integral is of *Airy* form and accounts for the contribution $\Gamma(1/3)$ in Eq. (2.36). More importantly, when this integral is performed, the small parameter ϵ scales out and contributes a factor of $\epsilon^{-1/6}$. This factor combines with the factor of $\epsilon^{-1/2}$ in Eq. (2.39) to give a factor of $\epsilon^{-2/3}$, which is precisely the asymptotic result in Eq. (2.36). The vanishing eigenvalue corresponds in the language of catastrophe theory to a coalescence of saddle

TABLE II. To verify the accuracy of the strong-coupling perturbation series, numerical values of the one-point and two-point Green's functions G_1 and G_2 at $g=1$ are obtained from the first four orders of the strong-coupling expansion for the case $D=1$. (The blank spaces in the table correspond to the appearance of complex numbers in the Padé extrapolants.) The numerical values of G_1 in the table must be multiplied by i. The exact values of the Green's functions were obtained by direct numerical integration of the Schrödinger equation. Three theories are considered here: $\alpha=3$ gives an $i\phi^3$ theory, $\alpha=4$ gives a $-\phi^4$ theory, and $\alpha=5$ gives a $-i\phi^5$ theory.

$\alpha=3$	Order 1	Order 2	Order 3	Order 4	Exact	Error (%)
G_1	-0.66835	-0.65587	-0.65016	-0.64718	-0.64058	1.02
G_2	-0.44669	-0.43017	-0.42271		-0.40944	3.14
$\alpha=4$						
G_1	-1.03865	-1.01113	-0.99836	-0.99150	-0.97347	1.82
G_2	-0.32956	-0.31603	-0.30887		-0.29473	4.58
$\alpha=5$						
G_1	-1.24289	-1.20721	-1.19067	-1.18167	-1.15497	2.26
G_2	-0.23702	-0.22935	-0.22351		-0.21043	5.85

points. This coalescence is associated with the matching at the distant turning point t_2 in the WKB calculation in Sec. II C.

III. STRONG-COUPLING CALCULATION OF G_1

In this section we perform a strong-coupling (large-g) calculation of the one-point Green's function G_1. The graphical methods for lattice strong-coupling techniques that we use here are explained in detail in a series of papers [24–27]. In the strong-coupling regime we can neglect the mass term in the Lagrangian (1.5). Because strong-coupling graphical methods are extremely general, we consider the one-parameter family of Lagrangian densities

$$\mathcal{L}=\frac{1}{2}(\nabla\phi)^2-\frac{1}{\alpha}g(i\phi)^\alpha, \tag{3.1}$$

where we recover the massless version of Eq. (1.5) when $\alpha=4$.

We obtain the graphical rules for the lattice strong-coupling expansion by observing that in the limit of large g the kinetic term in the Lagrangian density $\mathcal{L}$ in Eq. (3.1) can be viewed as a small perturbation. Therefore, the vacuum persistence amplitude $Z[J]$ [see Eq. (2.2)] for the quantum field theory associated with $\mathcal{L}$ can be factored as

$$Z[J]=\exp\left[\frac{1}{2}\int d^Dx\,d^Dy\,\frac{\delta}{\delta J(x)}\Delta^{-1}(x-y)\frac{\delta}{\delta J(y)}\right]Z_0[J], \tag{3.2}$$

where $\Delta^{-1}(x-y)=\nabla^2\delta^D(x-y)$ is the inverse of the free massless propagator in coordinate space and

$$Z_0[J]=\int_C\mathcal{D}\phi\exp\left\{\int d^Dx\left(\frac{1}{\alpha}g[i\phi(x)]^\alpha+J(x)\phi(x)\right)\right\}. \tag{3.3}$$

TABLE III. Numerical values of the one-point and two-point Green's functions G_1 and G_2 at $g=1$ obtained from the first four orders of the strong-coupling expansion for $0\leqslant D\leqslant 2$. The numerical values of G_1 in the table must be multiplied by i. Three theories are considered here: $\alpha=3$ gives an $i\phi^3$ theory, $\alpha=4$ gives a $-\phi^4$ theory, and $\alpha=5$ gives a $-i\phi^5$ theory.

	$\alpha=3$		$\alpha=4$		$\alpha=5$	
D	G_1	G_2	G_1	G_2	G_1	G_2
0	-0.72901	-0.53146	-0.97774	-0.28000	-1.07865	-0.16434
0.2	-0.70266	-0.50241	-0.97353	-0.28195	-1.08776	-0.17088
0.4	-0.67827	-0.47837	-0.97081	-0.28437	-1.10190	-0.17928
0.6	-0.65732	-0.46447	-0.97294	-0.28951	-1.12157	-0.19014
0.8	-0.64920	-0.43739	-0.98097	-0.29739	-1.14702	-0.20440
1.0	-0.64718	-0.42271	-0.99150	-0.30887	-1.18167	-0.22351
1.2	-0.63956	-0.41225	-1.00904	-0.32523	-1.22953	-0.24982
1.4	-0.63745	-0.40670	-1.03683	-0.34841	-1.29727	-0.28743
1.6	-0.64404	-0.40704	-1.08005	-0.38148	-1.39669	-0.34400
1.8	-0.66707	-0.41481	-1.15123	-0.42960	-1.55066	-0.43532
2.0	-0.65751	-0.43231	-1.27438	-0.50188	-1.80942	-0.59834

The factorization in Eq. (3.2) of the vacuum persistence function leads to the strong-coupling lattice expansion. By introducing a D-dimensional hypercubic lattice with lattice spacing a we rewrite Eq. (3.3) as a product of ordinary integrals over lattice sites k:

$$Z_0[J]=\prod_k \int_C dt\,\exp\left[\frac{1}{\alpha}a^D g(it)^\alpha + a^D J_k t\right]. \tag{3.4}$$

To obtain the vertices we expand the one-dimensional integrals as series in powers of J:

$$\mathcal{Z}_0[J]=\prod_k \sum_{n=0}^{\infty}\frac{1}{n!}(a^D J_k)^n \int_C dt\, t^n \exp\left[\frac{1}{\alpha}a^D g(it)^\alpha\right].$$

Next, we evaluate each of the one-dimensional integrals by deforming the contour C so that it enters the origin along a ray in the left-half t plane at the angle $-\pi/2-\pi/\alpha$ and leaves the origin along a ($\mathcal{PT}$-reflected) ray in the right-half t plane at the angle $-\pi/2+\pi/\alpha$. Each integral can now be expressed in terms of a Gamma function. To identify the vertices we write $\mathcal{Z}_0[J]$ in the form

$$\mathcal{Z}_0[J]=\mathcal{N}\exp\left\{a^D\sum_i\left[\sum_{n=1}^{\infty}\frac{1}{n!}J_i^n V_n\right]\right\},$$

where $\mathcal{N}$ is a multiplicative numerical constant. The vertices V_n have the form

$$V_n = a^{D(n-1)}(a^D g)^{-n/\alpha} v_n \quad (n\geq 1),$$

where v_n are numerical constants. The first three of the v_n are

$$\begin{aligned}
v_1 &= -2\,i\,\alpha^{1/\alpha}\cos(\pi/\alpha)\,\Gamma(2/\alpha)/\Gamma(1/\alpha),\\
v_2 &= n^{2/\alpha}\{4\cos^2(\pi/\alpha)\,\Gamma^2(2/\alpha)\\
&\quad -[1+2\cos(2\pi/\alpha)]\,\Gamma(1/\alpha)\,\Gamma(3/\alpha)\}/\Gamma^2(1/\alpha),\\
v_3 &= 2\,i\,\alpha^{3/\alpha}\cos(\pi/\alpha)\{8\cos^2(\pi/\alpha)\,\Gamma^3(2/\alpha)\\
&\quad -3[1+2\cos(2\pi/\alpha)]\,\Gamma(1/\alpha)\,\Gamma(2/\alpha)\,\Gamma(3/\alpha)\\
&\quad +2\cos(2\pi/\alpha)\,\Gamma^2(1/\alpha)\,\Gamma(4/\alpha)\}/\Gamma^3(1/\alpha).
\end{aligned} \tag{3.5}$$

The propagator on the lattice can be written in vector notation as $\Delta^{-1}=a^{-D-2}[(\underline{1})-2D(\underline{0})]$. This notation was introduced in Ref. [25], where this discrete form of the propagator was used to evaluate lattice integrals, which become sums over Kronecker delta functions on the hypercubic lattice. The lattice strong-coupling expansion is organized according to the number of free propagators Δ^{-1} (in contrast to weak-coupling expansions where the number of *vertices* and not the number of lines determines the order).

After calculating to a given order in perturbation theory we use Padé methods to extrapolate to the continuum limit ($a\to 0$). The results at $D=1$ for the one- and two-point Green's functions to fourth order in the strong-coupling expansion are shown in Table II. These results are in superb agreement with the exact values of the Green's functions obtained by numerical solution of the Schrödinger equation. These numerical calculations are explained in Ref. [7] where they were performed to check the accuracy of variational calculations. For other Euclidean dimensions $0\leq D\leq 2$ the numerical values of these Green's functions are given for the cases $\alpha=3,4,5$ in Table III. These are new field theoretical results.

ACKNOWLEDGMENTS

We thank the U.S. Department of Energy for financial support.

[1] F. J. Dyson, Phys. Rev. **85**, 631 (1952).
[2] C. M. Bender and T. T. Wu, Phys. Rev. Lett. **21**, 406 (1968).
[3] C. M. Bender and T. T. Wu, Phys. Rev. **184**, 1231 (1969).
[4] C. M. Bender and S. Boettcher, Phys. Rev. Lett. **80**, 5243 (1998).
[5] C. M. Bender, S. Boettcher, and P. N. Meisinger, J. Math. Phys. **40**, 2201 (1999).
[6] C. M. Bender and S. Boettcher, J. Phys. A **31**, L273 (1998).
[7] C. M. Bender, F. Cooper, P. N. Meisinger, and V. M. Savage, Phys. Lett. A **259**, 224 (1999).
[8] C. M. Bender, S. Boettcher, H. F. Jones, and V. M. Savage, J. Phys. A **32**, 1 (1999).
[9] C. M. Bender, G. V. Dunne, and P. N. Meisinger, Phys. Lett. A **252**, 272 (1999).
[10] A. A. Andrianov, M. V. Ioffe, F. Cannata, and J.-P. Dedonder, Int. J. Mod. Phys. A **14**, 2675 (1999).
[11] E. Delabaere and F. Pham, Phys. Lett. A **250**, 25 (1998); **250**, 29 (1998).
[12] E. Delabaere and D. T. Trinh, ''Spectral Analysis of the Complex Cubic Oscillator,'' University of Nice report, 1999.
[13] M. Znojil, Phys. Lett. A **259**, 220 (1999).
[14] C. M. Bender and G. V. Dunne, J. Math. Phys. **40**, 4616 (1999).
[15] F. Cannata, G. Junker, and J. Trost, Phys. Lett. A **246**, 219 (1998).
[16] A detailed discussion of the rotation of contours for eigenvalue problems is given in C. M. Bender and A. Turbiner, Phys. Lett. A **173**, 442 (1993).
[17] C. M. Bender and K. A. Milton, Phys. Rev. D **55**, R3255 (1997). A factor of 2 error appears in Eqs. (15) and (16) in this reference.
[18] C. M. Bender and K. A. Milton, Phys. Rev. D **57**, 3595 (1998).
[19] C. M. Bender and K. A. Milton, J. Phys. A **32**, L87 (1999).
[20] C. M. Bender and H. F. Jones, ''Effective Potential for $\mathcal{PT}$-Symmetric Quantum Field Theories,'' Found. Phys. (to be published).
[21] C. M. Bender, K. A. Milton, and V. M. Savage, ''Solution of Schwinger-Dyson Equations for $\mathcal{PT}$-Symmetric Quantum Field Theory.''
[22] C. M. Bender and S. A. Orszag, *Advanced Mathematical Methods for Scientists and Engineers* (McGraw-Hill, New York, 1978), Chap. 6.

[23] *Handbook of Mathematical Functions*, Natl. Bur. Stand. Appl. Math. Ser. No. 55, edited by M. Abramowitz and I. A. Stegun (U.S. GPO, Washington, D.C., 1965), Chap. 10.
[24] C. M. Bender, F. Cooper, G. S. Guralnik, H. Moreno, R. Roskies, and D. H. Sharp, Phys. Rev. Lett. **45**, 501 (1980).
[25] C. M. Bender, F. Cooper, G. S. Guralnik, R. Roskies, and D. H. Sharp, Phys. Rev. D **23**, 2976 (1981).
[26] C. M. Bender, F. Cooper, G. S. Guralnik, R. Roskies, and D. H. Sharp, Phys. Rev. D **23**, 2999 (1981).
[27] C. M. Bender, F. Cooper, G. S. Guralnik, R. Roskies, and D. H. Sharp, Phys. Rev. D **24**, 2683 (1981).